ROCK FRACTURE DYNAMICS RESEARCH AT AECL'S UNDERGROUND RESEARCH LABORATORY: APPLICATIONS TO GEOLOGICAL DISPOSAL OF RADIOACTIVE WASTE

R.P. Young
University of Toronto
Toronto, Ontario, Canada

J.R. Haycox
Applied Seismology Consultants Limited
Shrewsbury, Shropshire, United Kingdom

J. Martino
Atomic Energy of Canada Limited
Pinawa, Manitoba, Canada

ABSTRACT

Studies of rock fracture dynamics at AECL's Underground Research Laboratory (URL) have helped to provide a fundamental understanding of how crystalline rock responds to stresses induced from excavation, pressurization and temperature changes. The data acquired continue to provide insights into how a facility for the future geological disposal of radioactive waste could be engineered. Research into microseismic (MS), acoustic emission (AE), and ultrasonic velocity measurements has been performed on the full-scale sealed, pressurized, and heated horizontal elliptical tunnel at the Tunnel Sealing Experiment (TSX). The continuous monitoring of the experiment for 8 years provides a unique dataset for the understanding of the medium-term performance of an engineered disposal facility.

This paper summarizes the results, interpretations and key findings of the experiment paying particular focus to the heating and cooling/depressurization of the chamber. Initial drilling of the tunnel and bulkheads causes microfracturing around the tunnel, mapped by MS and AEs, and is used as a benchmark for fracturing representing the excavated damaged zone (EDZ). There is no further extension to the volume during pressurization or heating of the tunnel suggesting an increase in crack density and coalescence of cracks rather than extension into unfractured rock. The dominant structure within the seismic cloud has been investigated using a statistical approach applying the three-point method. MS events in the roof exhibit a dominant pattern of sub-horizontal and shallow-dipping well defined planar features, but during cooling and depressurization a 45 degree dip normal to the tunnel axis is observed, which may be caused by movement in the rock-concrete interface due to differential cooling of the bulkhead and host rock. Cooling and depressurization of the TSX have not led to a significant increase in the number of MS or AE events. Ultrasonic results suggest the rock gets even stiffer in the first months of cooling, but this is slowly reduced towards the end of the experiment as microfractures reopen possibly also caused by a relaxation of the rock as the chamber depressurizes. AEs located at the concrete bulkhead delineated three macrofracture zones during curing. The high-resolution locations were used to delineate and monitor the growth of the fault plane allowing focused injection of grout to heal the developed damage.

1. INTRODUCTION

Research into induced microseismicity was conducted at AECL's Underground Research Laboratory (URL) for 20 years between 1987 and 2007 to investigate the rock mechanical and geotechnical aspects of the safe geological disposal of radioactive waste [1]. Passive monitoring of events induced in rocks subject to stress changes imposed by tunnels and engineered structures provides a unique means of monitoring the effect of the treatment and the changes imposed on the fracture network. Induced seismicity has been used in the Mineby experiment [2,3,4], Heated Failure Test [4,5] and Excavation Stability Study as part of comprehensive geomechanical and hydrological experiments. This has led to an improved understanding of excavation response that is particularly relevant when long-term geologic isolation of nuclear waste is considered [1].

This paper looks in detail at the findings from microseismic (MS), acoustic emission (AE) and ultrasonic monitoring of the Tunnel Sealing Experiment (TSX); a major international experiment at the URL conducted to address construction and performance issues of full-scale seals for potential application to deep geological disposal facilities for radioactive waste [6]. Previous studies at the TSX have presented results during excavation of the tunnel [7] and pressurization of the chamber [8]. This paper summarizes the results, interpretations and key findings of the experiment paying particular focus to the heating and cooling/depressurization of the chamber in 2003 and 2004.

2. BACKGROUND

2.1 The Underground Research Laboratory

The Underground Research Laboratory (URL) was a facility established by Atomic Energy of Canada Ltd. (AECL) in Manitoba. The URL's main objective was to study the feasibility of safe disposal of nuclear fuel in a stable excavation in a low permeability rock mass. One of the most important aspects is the investigation of the rock mechanical and geotechnical aspects of the safe geological disposal of radioactive waste. It represented a unique facility to study the fundamental behavior of initially unfractured granite in-situ. The facility consisted of a 443-m deep shaft, a ventilation shaft and two main experimental levels, the 240 and 420 Levels.

2.2 The Tunnel Sealing Experiment

The Tunnel Sealing Experiment (TSX) was a major international experiment conducted at the URL to address construction and performance issues of full-scale seals for potential application to deep geological disposal facilities for radioactive waste [9]. Bulkheads and plugs, used to isolate waste packages and to seal the entrances to repositories, are an important element in the concepts advanced by many international organizations charged with the management of radioactive waste. In the Environmental Impact Statement (EIS) outlining the Canadian concept for disposal of Canada's nuclear waste [10], seals are used to keep the buffer and containers in place, retard the movement of contaminants released from the containers and to isolate tunnels and shafts from the biosphere.

The TSX comprised two full-scale tunnel bulkheads keyed into the rock mass separated by a sand filed tunnel that was pressurized: one composed of clay blocks and the other constructed using low-heat high-performance concrete (LHHPC). The 'clay' bulkhead consisted of 9,000 highly compacted bentonite-sand based bricks. An AE system was installed in the rock volume around the bulkhead. A second AE system was installed inside the concrete bulkhead using a glass fibre frame. Passive and active monitoring was performed during the curing process, identifying the occurrence of cracks, investigating the extent to which these cracks were stabilized through remedial grouting and allowing the study of the long-term behavior of the bulkhead. The geophysical data were processed using InSite seismic processor, a commercially available software package developed to include a data capture facility, real-time processor and distributed-user functions and quality assurance system for calibration of processing algorithms [11].

3. PROCESSING METHODOLOGY

3.1 MS Instrumentation

The MS system consisted of 16 triaxial accelerometer sensors that cover a region of approximately 100,000 m^3 centered around the TSX chamber. The sensors were sensitive to frequencies in the 0.1 to 10 kHz band. Monitoring using this system was undertaken daily between December 1996 and March 2007. The system generally monitored for 16 hours each weekday (off between 08:00 and 16:00 during working hours). Source locations and seismic source parameters were calculated using the automated method described in [12]. The source parameter values calculated include estimates of the magnitude and energy content (seismic moment and radiated energy); stress release (apparent stress); source dimension assuming a circular source model, and the ratio of energy in the P and S-wave (E_S/E_P) which is a useful parameter for source mechanism analysis.

A calibration study to ascertain location accuracy has been performed [13]. This procedure entailed creating artificially-induced seismic events with an impact hammer source in rooms of the 420m level. The coordinates of these events were surveyed. A source seismic moment of $\sim 1\times 10^5$ Nm is produced using this method, comparable to the largest events recorded in the Mine-by experiment [14]. The minimum error is 0.5 m following P- and S-wave velocity calibration.

3.2 TSX Instrumentation

Two AE systems monitored the bulkheads at the TSX. The concrete bulkhead consisted of an array of 24 ultrasonic transducers installed within the concrete key and the surrounding rock mass. Sixteen of the transducers are used to record passive AE events and the active velocity surveys. The remaining 8 transducers are used as the sources for the active velocity surveys. The system to monitor the clay bulkhead had a similar configuration, with 16 uniaxial receiving transducers installed along 4 boreholes. A transmitting transducer is also installed at the end of each borehole and 4 transmitting transducers are installed on the NE sidewall. Automatic daily velocity surveys were performed at 01:00 hours. The velocity surveys are processed using a cross-correlation method [15] and maximum peak-to-peak amplitudes calculated within a defined picking window. Changes in amplitude and velocity along raypaths can be interpreted in terms of local changes in the rock properties.

4. RESULTS AND INTERPRETATIONS

4.1 MS Results and Interpretations

4.1.1 MS Locations at the URL

MS locations for the period between January 1998 and March 2005 are presented in Figure 1. This covers the time after excavation of the TSX tunnel and bulkhead keys. The 5,806 events are colored to a time scale. Most of the tunnels of the 420 Level are associated with some level of activity. In some cases clusters of events can be recognized along tunnels which could be caused by induced stresses present around irregularities of the tunnel or lithological variations. Adjacent tunnels show continued activity in the roof and floor which could possibly be due to induced stress from the TSX excavation. Stress magnitudes and orientations (given as trend/plunge) are σ_1 = 60 ± 3 MPa (145°/11°); σ_2 = 45 ± 4 MPa (054°/08°); σ_3 = 11 ± 2 MPa (290°/77°), where σ_1, σ_2, and σ_3 are the maximum, intermediate and minimum principal stresses respectively [16]. The two green lines of events (marked 'A' in Figure 1) are instrumentation cable holes to access the TSX chamber and are probably displaying breakout activity delineating their trajectory.

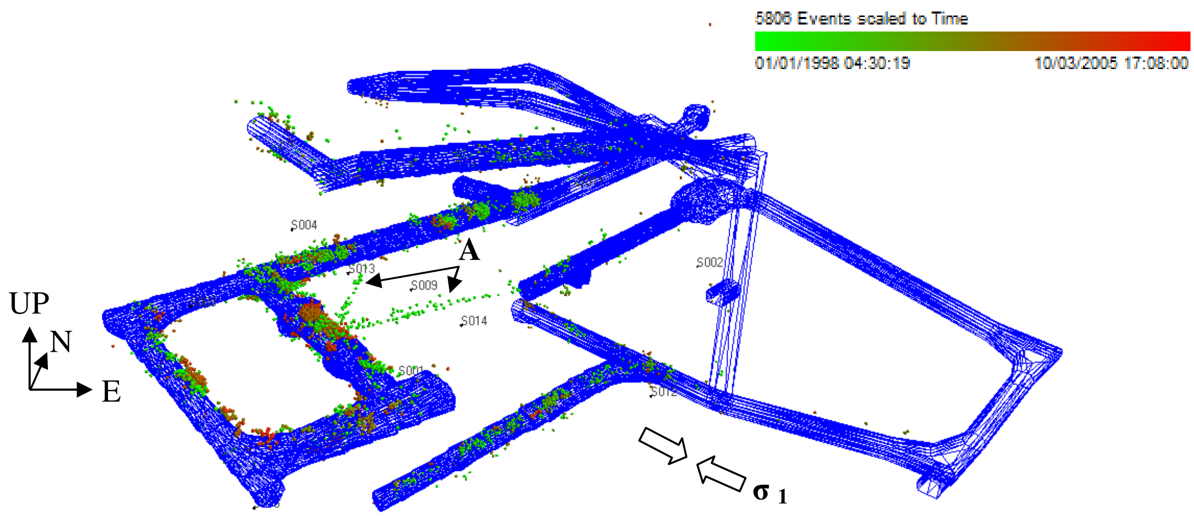

Figure 1. MS events recorded post-excavation of TSX tunnel and bulkhead keys between 1 January 1998 and 6 June 2006. The events are colored according to a time scale (green early, red late).

4.1.2 <u>MS Locations at the TSX</u>

Studies have previously been carried out on MS events occurring in the region around the TSX bulkheads during the excavation and pressurization of the tunnel [7,8]. Observing patterns of MS events around the chamber for various phases of the TSX allows a better understanding of the processes of microfracturing occurring. Figure 2 shows plan and side views of room 425 and associated MS activity for various phases of the TSX. Initial excavation of the tunnel induced intense MS activity. The relative location of a subset of these events using a set of surveyed man-made master events showed that the damage zone is constrained to the first 0.6 m from the tunnel free surface in the floor region and to the first 1 m in the roof region [17]. Seismic activity ceased in the floor after 0.05–0.1 MPa of confining pressure was placed on the floor region of the tunnel perimeter, and ceased in the roof when under 2 MPa of hydraulic pressure. [8]. The additional pressure applies a confining pressure to the rock adjacent to the chamber restricting the growth or movement of fractures [8].

During temperature increase in the room, the number of events increases. The activity is likely to be caused by heating of water in microcracks of the Excavation Damaged Zone (EDZ) around the chamber. As the temperature of the water increases it expands causing movement on or extension of pre-existing microcracks and increased hydraulic pressure, particularly in the first metre of rock, due to thermal expansion of trapped porewater [6]. During cooling and depressurization events are observed to occur around the floor and roof of the tunnel. Activity is also observed around the bulkheads which could be the result of differential cooling of the bulkhead material relative to the surrounding rock.

Figure 2 can also be used to assess changes to the distribution of MS events, equivalent to variations in the extent of the EDZ. Over 7 years the events do not appear to locate further from those MS events recorded during the initial excavation of the tunnel. The spatial distribution of the MS events is constrained to 2.8 m distance from the tunnel wall in a region between the bulkheads. The average distance from the chamber wall is 0.74 m and over 95% of the events are located less than 1.40 m away. This has implications to the size and development of the EDZ. The results show that the MS events that occur during heating do not extend further than 2 m from the chamber wall, which is no further than the microcracking induced by tunnel and key excavations. Therefore it can be interpreted that fracturing of the virgin rock beyond the initial EDZ is unlikely to be occurring. Extension of existing microcracks or an increase in the density of cracks is more likely. Confinement of the microcracks in the lower half of the tunnel explains why the events are located closer to the tunnel wall during heating (less than 1.3 m). A gap in MS events appears to exist near the bulkheads. This could be caused by changes to the stress conditions where the keys extend into the rock. The roof of the chamber is not confined by the weight of sand resulting in MS activity continuing in the roof over a longer period.

4.1.3 Fracture Geometry from MS Events

This study has employed an approach to interpret the induced fracture network by using information on fracturing mode and orientation from the microseismic catalogue. The method is based on the statistical analysis of event locations to determine the dominant structure defined within the seismic cloud. This is achieved using a statistical approach applying the three point method (e.g. [18,19,20]). This technique has previously been employed for MS events located during excavation of the TSX tunnel [18]. Figure 3a shows density stereonets of pole distribution for planes fitted to triads of events for the whole excavation period. The key shows how positions on the stereonets relate to inferred fracture orientations around the tunnel. During excavation, MS events in the roof exhibit dominant pattern of sub-horizontal and shallow-dipping well defined planar features. These are at a tangent to the upper wall of the tunnel. The MS events in the floor show a similar pattern of sub-horizontal planar features but the envelope does not extend as far in the roof.

During heating of the TSX (Figure 3b), sub-horizontal features continue to be defined in the roof, with preferential poles to the NE. The plan view of events located during heating (Figure 2F) shows that the events are located towards the NE of the tunnel so this distribution is expected. Few events are located in the floor and no dominant structure is identified. The pole distribution does not display a different pattern to that observed during excavation suggesting that fracturing follows a trend initiated during excavation. A different trend is identified during cooling and depressurization in the roof with a dominant trend observed at 45 degree dip normal to the tunnel axis (Figure 3c). This could be interpreted as being caused by movement on the rock-concrete interface due to differential cooling of bulkhead and host rock. Events in the floor show poorly defined shallow-dipping sub-horizontal features.

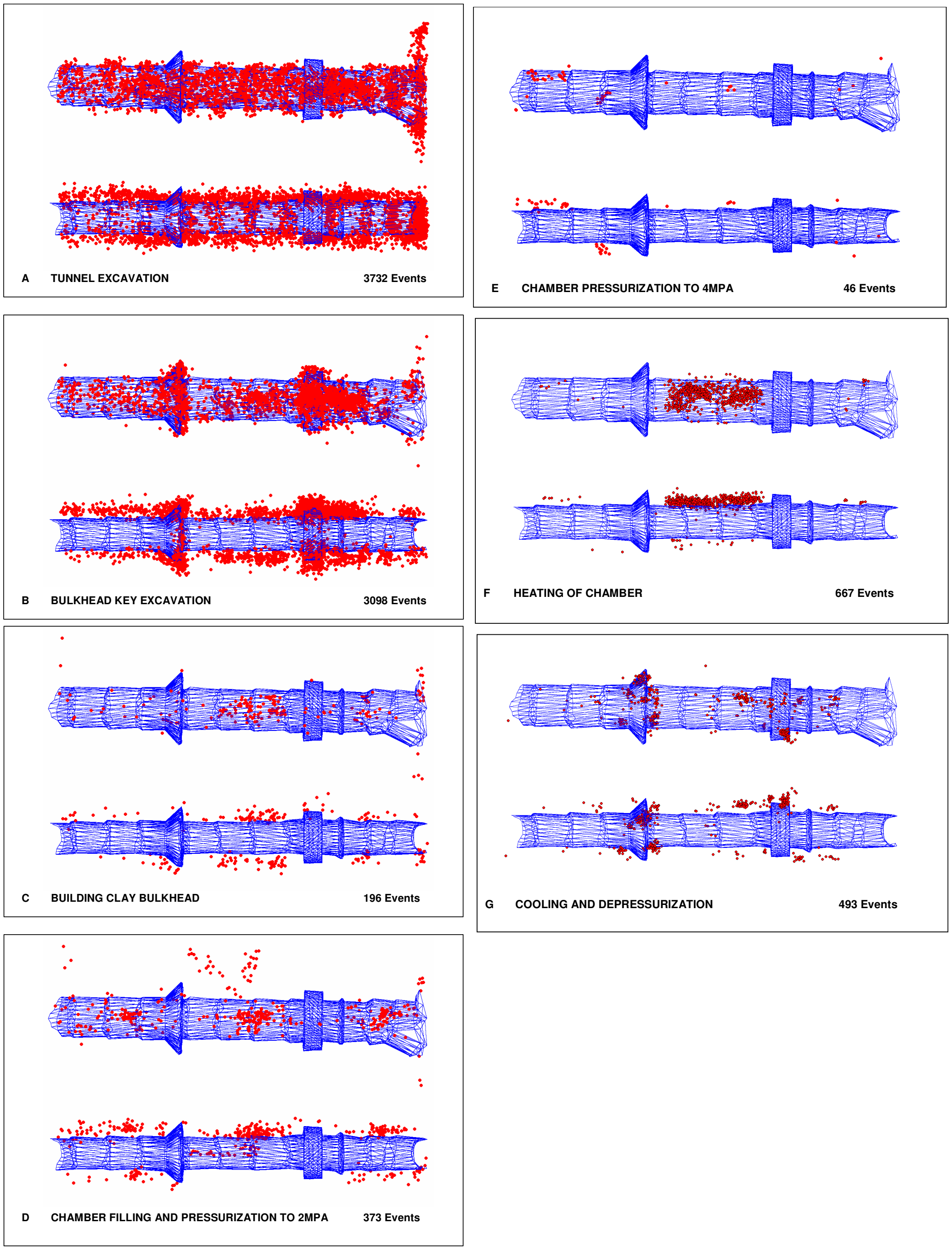

Figure 2. Spatial distribution of MS events from start of excavation showing activity around room 425 at different phases of the Tunnel Sealing Experiment. A) Tunnel Excavation: 18 January 1997 to 20 March 1997 12:00, B) Bulkhead Key Excavations: 20 March 1997 12:00 to 31 December 1997, C) Building Clay Bulkhead: 1 January 1998 to 8 July 1998, D) Chamber filling and Pressurization to 2 MPa: 9 July 1998 to 23 April 2001, E) Chamber Pressurization to 4 MPa: 24 April 2001 to 24 September 2002, F) Heating of Chamber: 25 September 2002 to 10 November 2003, G) Cooling and Depressurization: 11 November 2003 to 8 March 2005. Top plot in each pane is a plan view; bottom plot is a side view looking towards NE.

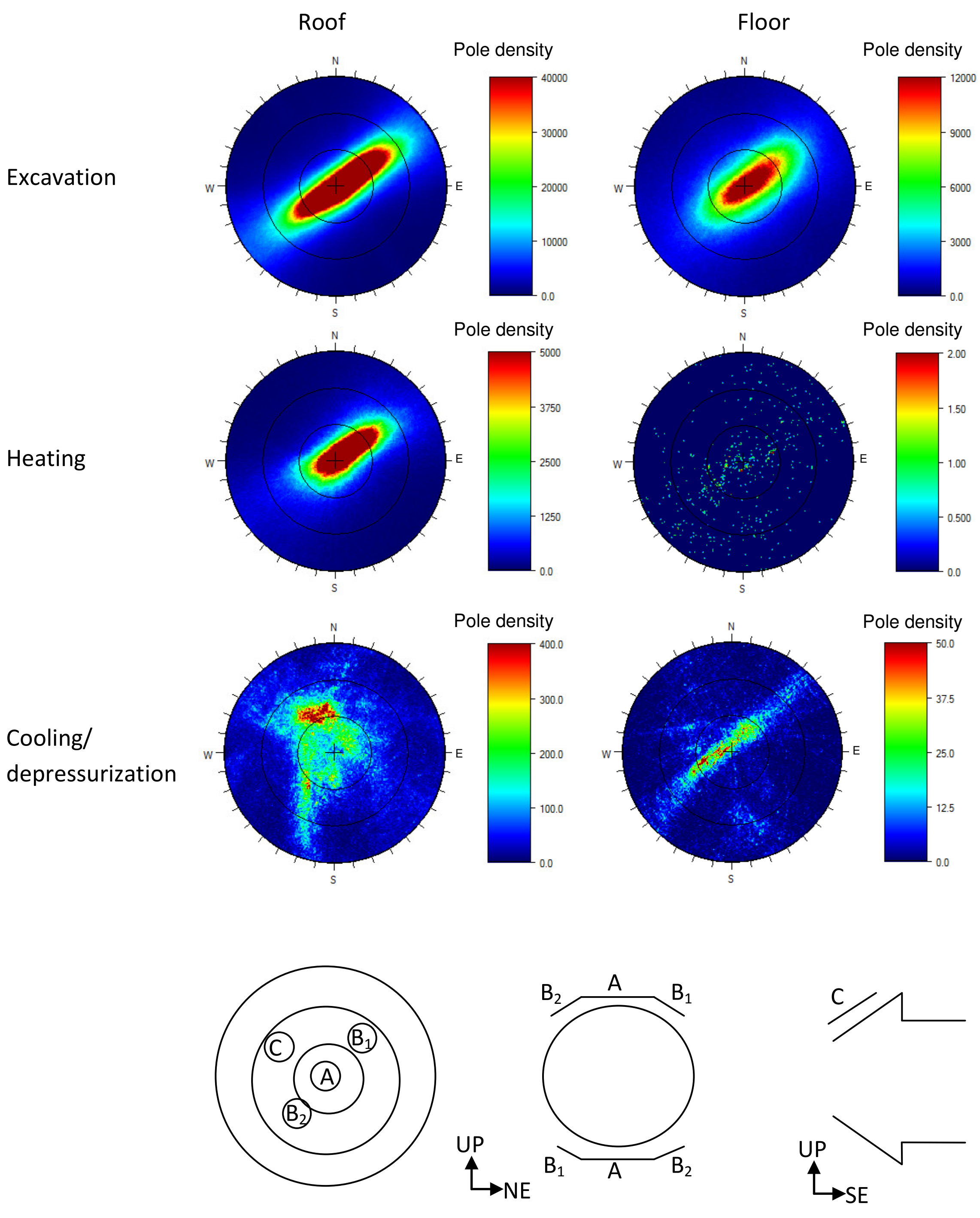

Figure 3. Density stereonets of pole distribution for planes fitted to triads of events. This shows the evolution of the dominant structure of the induced fracture-network interpreted from the location of the microseismic events located during three periods. Top) Tunnel Excavation: 18 January 1997 to 20 March 1997 12:00; Middle) Heating of Chamber: 25 September 2002 to 10 November 2003; Bottom) Cooling and Depressurization: 11 November 2003 to 8 March 2005. Stereonets on the left are for events in the roof of the tunnel and stereonets on the right are for events in the floor of the tunnel. Interpretation of pole density diagrams is presented at the bottom of the figure. Stereonets are northern hemisphere projections.

4.2 Clay Bulkhead AE and Ultrasonic Results and Interpretations

Figure 4 presents the locations of AE data recorded between July 1997 and July 2004 in the volume below the clay bulkhead at the TSX. The data is divided into five periods corresponding to those events recorded during (a) the excavation of the clay key and construction of the clay bulkhead, (b) the pressurization of the chamber, (c) the constant pressure stage, (d) the heating stage and (e) the cooling and depressurization stage. The array was configured to monitor the tunnel floor and rock under the bulkhead. Over the 7-year period of monitoring there are a total of 25,341 located AEs around the clay bulkhead. Approximately 86% of all the events are recorded during the excavation stage, as previously reported by [7]. The location of AEs during this period has been used as a benchmark for fracturing and can be interpreted as forming the EDZ.

This study compliments the previous observations with results from pressurization, heating and cooling/depressurization. Less than 1% of the total events occur during the pressurization stage, with no events locating below the TSX chamber after the pressure is increased above 2MPa. This suggests that the pressurization is acting to confine the rock around the tunnel, and is a method of stopping time-dependent microcracking from occurring around the tunnel perimeter. During the year of constant pressure in the chamber, 0.1% of the total events occur, with no events below the chamber apart from two isolated events locating 1-2 meters from the chamber perimeter. During the heating phase 12% of the total events occur, with the majority locate directly under the chamber. The AEs could mean that new microcracks are forming or existing microcracks are reactivated or propagated. It is noticed that the extent of the microcracked region during the heating phase is not beyond the extent of microcracking observed during the excavation phase, suggesting an increase in crack density and coalescence of microcracks rather than extension into unfractured rock. The majority of the events which occur during cooling and depressurization locate in a cluster under the clay bulkhead (the array geometry means that events would not be detected in the roof, but could be detected in the walls). These may be caused by the contraction of the rock around the bulkhead as it cools.

Ultrasonic results from around the clay bulkhead have previously been presented during excavation [7]. The dynamic Young's modulus (E) for two raypaths (6_13 and 4_8) has been calculated for the duration of the TSX (Figure 5). This encompasses the time between June 1997 when the system was installed and July 2004 when acquisition was terminated. Changes to the rock properties can therefore be observed in relation to major experimental activities. Figure 5a shows the result for a raypath from a transmitter in the tunnel wall. Three temporal changes in E are believed to be a result of temporary changes in temperature and humidity from the Evaporation Experiments carried out in that period. Ignoring these transient changes, it can be interpreted that: (i) an overall decrease of 3.5% in E occurs in the first year during which the clay key is excavated and the bulkhead is built; (ii) a decrease of about 1% occurs during the 3-year pressurization phase; (iii) a period of constant E occurs during the time that the chamber pressure is held constant, (iv) a 1% increase in E happens during the heating phase of the TSX, and (v) cooling causes E to increase by 1.5 % initially but drops off in the following few months. The convergence of E to a virtual constant value after 4 years suggests a stability in the rock mass was reached. The heating phase appears to cause an overall increase in the stiffness of the rockmass, back towards its undamaged/ undisturbed modulus value. The rock appears to get even stiffer in the first months of cooling, but this is slowly reduced towards the end of the experiment as microfractures reopen.

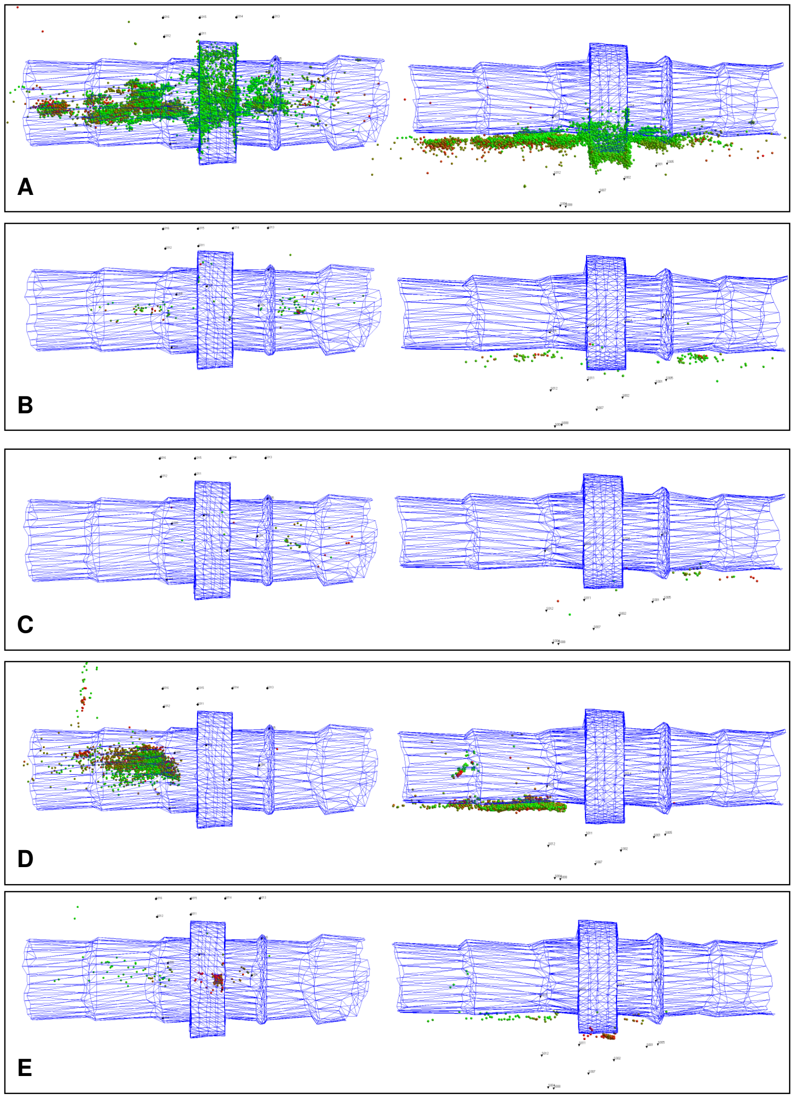

Figure 4. Spatial distribution of AEs since the clay system was installed. A) Excavation: June 1997 to September 1998, B) Pressurization: October 1998 to September 2001, C) Constant Pressure: October 2001 to September 2002, D) Heating: October 2002 to September 2003, E) Cooling and Depressurization: October 2003 to July 2004. Left plot is a plan view; Right plot is a side view looking NE. Events are color scaled to time for each period (green events early, red events late).

Figure 5b shows the results for a raypath from a borehole transmitter (raypath P4_R8). The data shows: (i) an increase of 0.5% in E during the clay key excavation and clay bulkhead construction; (ii) a decrease of 0.25% in E during the 3-year pressurization phase; (iii) no change in E during the constant pressure phase; (iv) an increase of 3% in E during the heating phase, and (v) a decrease in E of approximately 1% during cooling and depressurization. This raypath is believed to be outside of the damage zone around the TSX excavation. Therefore it is concluded that the rockmass at this distance from the tunnel is experiencing elastic (reversible) changes due to the stress effects of the excavation and construction activities and the pressure and temperature changes. Cooling would cause the rock at this distance to slowly relax causing preferentially aligned microfractures and pore spaces to slowly open. The change in E appears to be more closely related to depressurization of the chamber. As pressure in the chamber drops, surrounding rock may relax and cause reopening of microfractures. An increase of approximately 1.2% in Young's Modulus is observed since the start of pressurization in both Figure 5a and Figure 5b, probably caused by a closure of open fractures. This residual increase in modulus suggests that the rock has been permanently changed by the pressurization, heating, cooling, and depressurization cycle, although continued cooling may reduce this residual further.

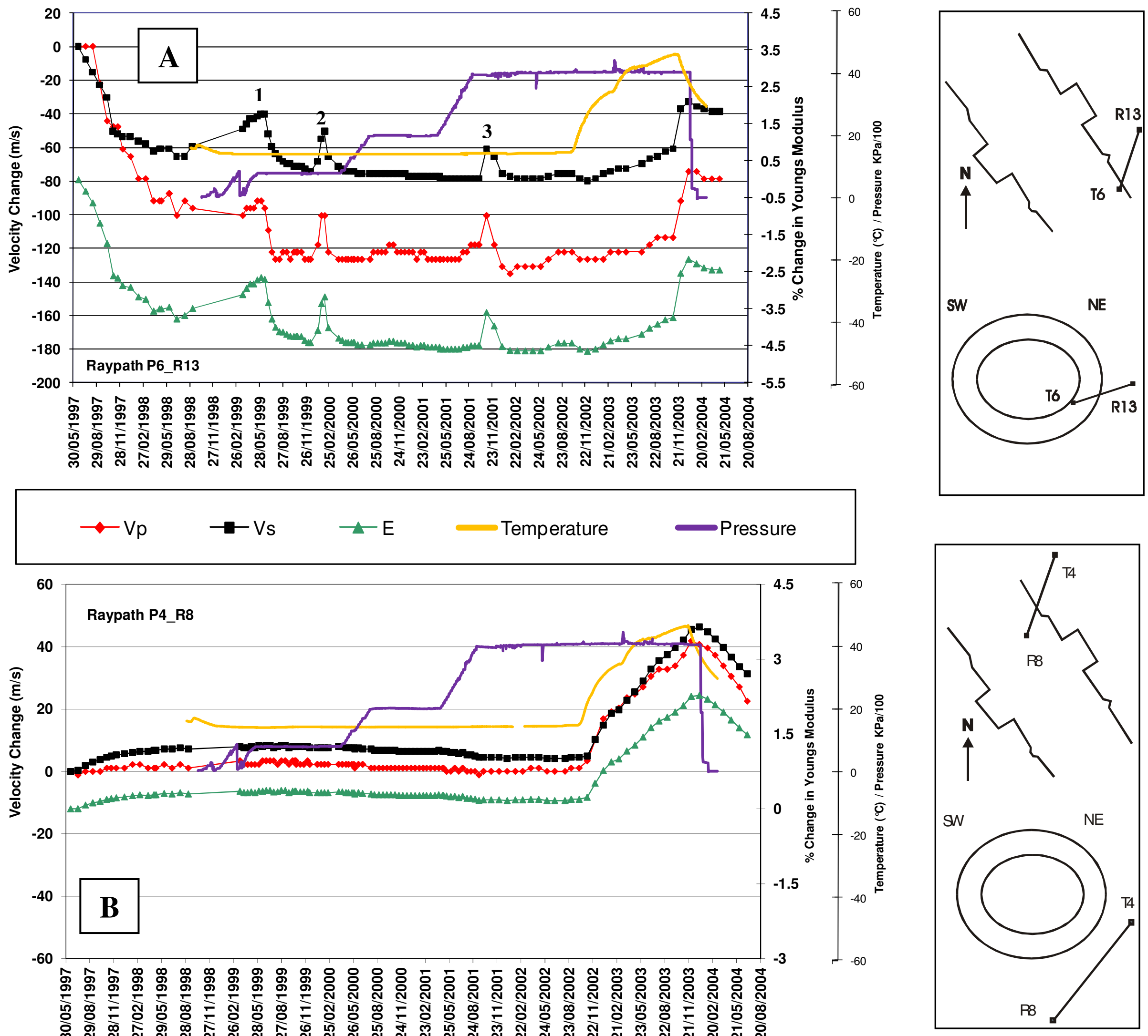

Figure 5. Change in P- and S-wave velocity and dynamic Young's Modulus over the 7 year time period that the AE System has been installed. Two raypaths are presented: A) Raypath 6_13 from tunnel transmitter to receiver, and B) Raypath 4_8 from borehole transmitter to receiver. The transient changes marked 1-3 are believed to be due to the Evaporation Experiment that was being performed.

4.3 Concrete Bulkhead Acoustic Emission and Ultrasonic Results and Interpretations

Figure 6 presents the locations of AE data recorded between September 1998 and April 2004. The data is divided into six periods corresponding to those events recorded during (a) the curing of the concrete bulkhead, (b) the post grouting interval, (c) the pressurization stage, (d) the constant pressure stage, (e) the heating stage, and (f) the current stage of cooling and depressurization. AE data has previously been presented and analyzed with results from other instrumentation [6]. An important finding from the AE results at the concrete bulkhead was the identification of 3 macrofracture zones during curing of the bulkhead. Approximately 84% of the total events were recorded in a one-month period of monitoring. The high-resolution location of AE events were used to delineate and monitor the growth of the fracture plane. These results allowed the injection of grout to be directed in order to heal the developed damage. Very few events locate in the following months of monitoring providing additional confirmation that the grouting had successfully filled the earlier induced fractures, and the bulkhead was acting as a whole unit. There is also no evidence for the formation of new macrofractures during pressure and temperature changes in the TSX chamber.

Ultrasonic survey results have been analyzed in the past for periods of curing [7]. A series of raypaths have been analyzed for the changes in P-wave velocity and amplitude over the 5-year period since the concrete bulkhead was poured. Velocity surveys occurring approximately every 1 to 2 weeks have been chosen for this analysis. Figure 7 shows P-wave velocity and amplitude from raypath P4_R9 across the bulkhead. The velocity and amplitude increase significantly from September 15-24th 1998, but the amplitude decreases virtually to zero following the occurrence of approximately 300 AE events over a 9-hour period. These AEs form a narrow slightly curved surface (2 x 4 m in length) which intersects the raypath, resulting in the pulsed waveform to be virtually completely attenuated by the resulting open fractures, and therefore no velocity determination was possible. Following the grouting phase, the velocity and amplitude data suggest the fracture surface has been successfully bonded. The velocity is seen to increase until September 2002, where it shows a small decrease and then a steady increase during the heating phase. During cooling, P-wave velocity decreases while S-wave velocity remains constant, suggesting desaturation may be occurring. However, depressurization affects the velocity along raypath P5_R5 to a greater extent, most likely to be a result of its axial orientation.

5. CONCLUSIONS

Microseismic (MS), acoustic emission (AE) and ultrasonic monitoring of the Tunnel Sealing Experiment (TSX) has been performed to interpret changes in rock during excavation, pressurization, heating, cooling and depressurization. Observing patterns of MS events around the chamber for various phases of the TSX allows a better understanding of the processes of microfracturing. The key findings from the experiment are:

- Initial drilling of the tunnel and bulkheads causes microfracturing around the tunnel within a distance of 2.8 m from the tunnel's edge. The events occurring during heating locate within 2 m, indicating there is no further extension of the EDZ with time. Activity during the heating phase can be interpreted as new microcracks forming or existing microcracks being reactivated or propagated. The extent of the microcracked region during the heating phase is not beyond the extent of microcracking observed during the excavation phase, suggesting an increase in crack density and coalescence of cracks rather than extension into unfractured rock.

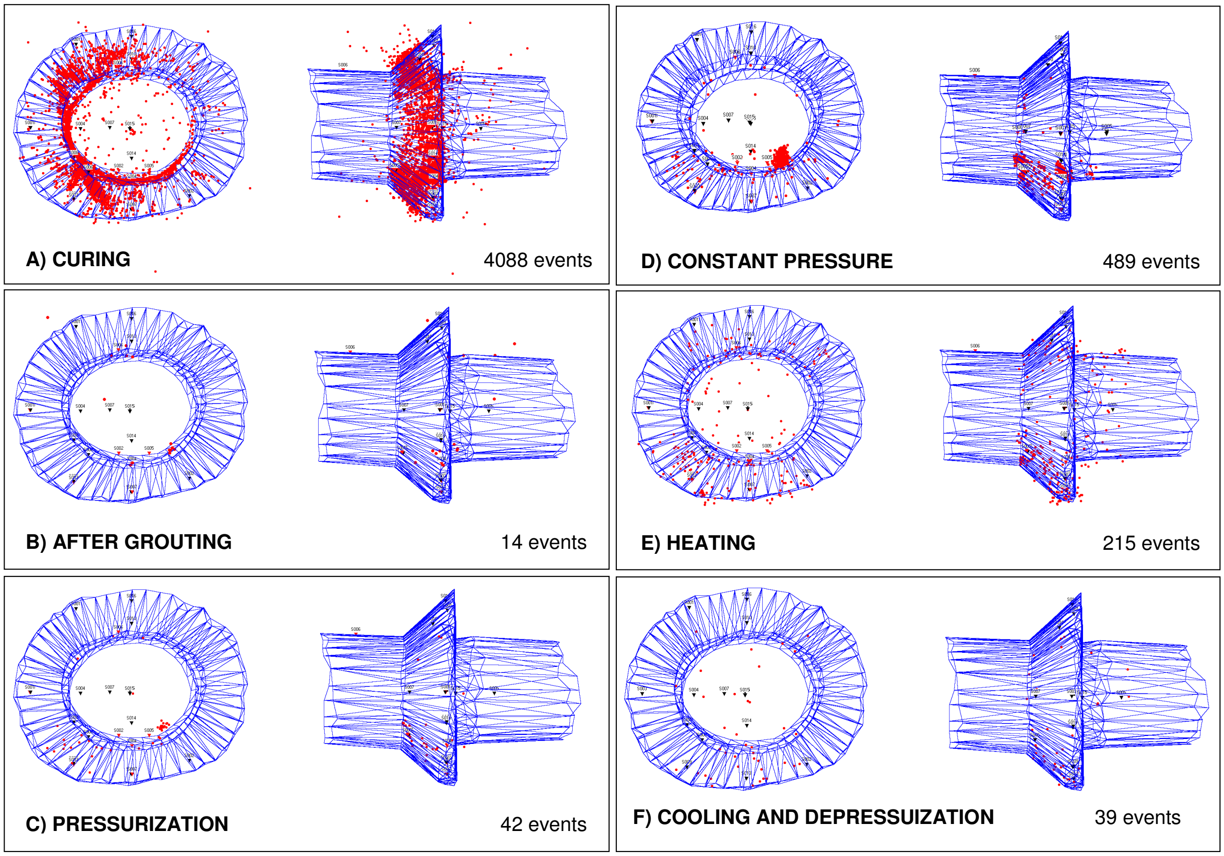

Figure 6. AE locations at the concrete bulkhead for two periods throughout the tunnel sealing experiment. A) Curing 16 September 1998 to 27 October 1998; B After Grouting: 1 February 1999 to 31 April 1999; C) Pressurization: 1 March 2001 to 30 September 2001; D) Constant Pressure: 1 October 2001 to 1 October 2002; E) Heating: 1 October 2002 to 30 September 2003, F) Cooling and Depressurization: 1 October 2003 to 15 April 2004. Left Plot is a Plan View; Right Plot is a Side View Looking NE.

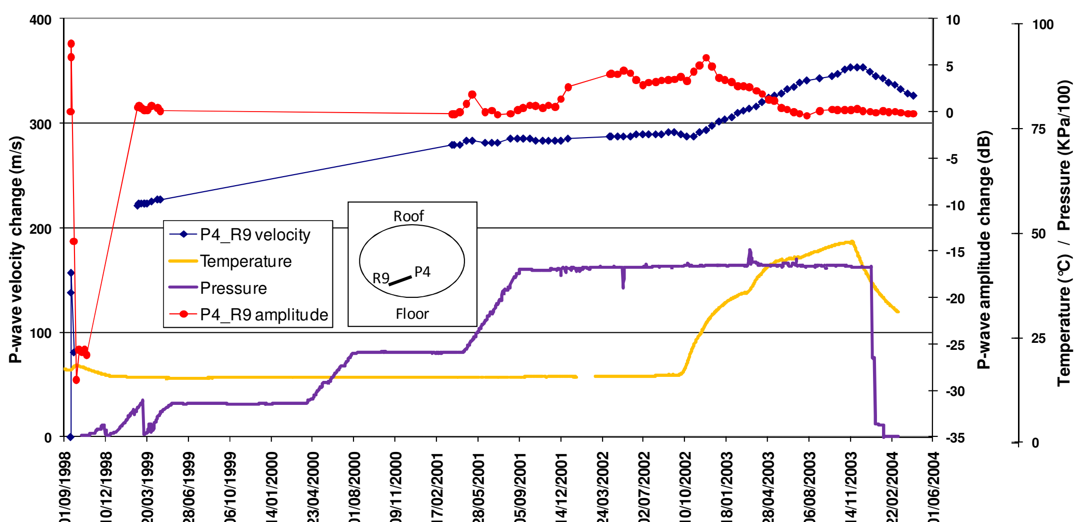

Figure 7. P-wave velocity and amplitude for raypath P4_R9 through the concrete bulkhead over a 5 year period of the TSX. The raypath passes through the region where a macrofracture formed in Phase 1 and a subsequently 'grouted'.

- The number of MS events in the upper half of the chamber is greater than in the floor region, a difference which can be partially due to the effect of gravity, however more investigation is required to fully understand this difference and the different confining pressures required to stop seismicity in the two regions. Numerical geomechanical models could provide further insight into this different behavior.
- The dominant structure within the seismic cloud has been investigated using a statistical approach applying the three-point method. MS events in the roof exhibit a dominant pattern of sub-horizontal and shallow-dipping well defined planar features during excavation which continue during heating, mapping post mortem and post excavation confirm tangential microfracturing. A different trend is identified during cooling and depressurization with a 45 degree dip normal to the tunnel axis observed, which is speculated to be caused by movement in the rock-concrete interface due to differential cooling of bulkhead and host rock. Events in the floor show shallow-dipping sub-horizontal features during excavation, while no clear structure is observed in later phases. The MS events in the floor show a similar pattern of sub-horizontal planar features but the envelope does not extend as far.
- Cooling and depressurization of the TSX did not lead to a significant increase in the number of MS or AE events. Ultrasonic results suggest the rock became even stiffer in the first months of cooling, but this is slowly reduced towards the end of the experiment as microfractures reopen. Further from the tunnel cooling causes the rock to slowly relax causing preferentially aligned microfractures and pore spaces to slowly open. The decrease in E appears to be more closely related to depressurization of the chamber. As pressure in the chamber drops, surrounding rock may relax and cause reopening of microfractures.
- AE events located at the concrete bulkhead occurred during a one-month period of monitoring during the curing stage with the majority of events delineating three macrofracture zones. The high-resolution location of AE events was used to delineate and monitor the growth of the fault plane. These results allowed directing the injection of grout in order to heal the developed damage; in the following two months of monitoring only a few events occur. Velocity and amplitude raypath data also suggest the fracture surface has been successfully bonded. Macrofractures identified during curing were not reactivated. There is also no evidence for the formation of new macrofractures associated to pressure and temperature changes in the TSX chamber. Velocity and amplitude changes are most dramatic during initial curing phase when an increase in both is observed.
- Dynamic Young's modulus has been calculated from ultrasonic surveys. Significant differences are observed between raypaths positioned at different regions of the rock. Following excavation, it took 4 years for Young's modulus in the tunnel wall to reach a virtual constant value suggesting stability in the rock mass was reached. The heating phase appears to cause an overall increase in the stiffness of the rockmass, back towards its undamaged/undisturbed modulus value. The rock appears to get even stiffer in the first months of cooling, but this is slowly reduced towards the end of the experiment as microfractures reopen. A raypath crossing a region further from the tunnel experiences elastic (reversible) changes due to the stress effects of the excavation and construction activities and the pressure and temperature changes.

Microseismic monitoring combined with active acoustic surveys as used at the URL is now an established technique employed in a wide range of disciplines and scales from hydraulic fracturing and reservoir monitoring in petroleum, enhanced geothermal systems, mining, carbon dioxide storage, civil engineering and laboratory testing. The research conducted at the URL continues to be important for the planning of future repositories for the disposal of radioactive waste worldwide.

6. ACKNOWLEDGEMENTS

The authors would like to thank Atomic Energy of Canada Ltd. for their scientific and financial support and permission to use the URL data. We also thank the TSX international project team, AECL, ANDRA/EDF, PNC and WIPP. We are grateful to personnel at the URL for their assistance with the MS and AE monitoring, backup, and maintenance. Thanks also to members of Young's research group over the years for their involvement and contributions to induced seismicity studies at the URL.

7. REFERENCES

[1.] Read, R.S. (2004). 20 years of excavation response studies at AECL's Underground Research Laboratory. *Int. J. Rock Mech. Min.*, **41**, 8, 1251–1275.

[2.] Baker, C. and Young, R.P. (1997). Evidence for Extensile Crack Initiation in Point Source Time-Dependent Moment Tensor Solutions. *Bull. Seis. Soc. America*, **87**, 6, 1442-1453.

[3.] Collins, D.S., and Young, R.P. (2000). Lithological Controls on Seismicity in Granitic Rocks. *Bull. Seis. Soc. America*, **90**, 3, 709-723.

[4.] Martino, J.B. and Chandler, N.A. (2004). Excavation-induced damage studies at the Underground Research Laboratory. *Int. J. Rock Mech. Min.*, **41**, 1413 – 1426.

[5.] Falls, S.D and Young, R.P. (1998). Acoustic Emission and Ultrasonic-Velocity Methods Used to Characterise the Excavation Disturbance Associated with Deep Tunnels in Hard Rock. *Tectonophysics*, **289**, 1-15.

[6.] Martino, J.B, Dixon, D.A, Kozak, E.T, Gascoyne, M., Vignal, B., Sugita, Y., Fujita, T. and Masumoto, K. (2007). The tunnel sealing experiment: An international study of full-scale seals. *Phys. Chem. Earth, Pt. A/B/C*, **32**, 1-7, 93-107

[7.] Young, R.P. and Collins, D.S. (2001). Seismic studies of rock fracture at the Underground Research Laboratory, Canada. *Int. J. Rock Mech. Min.*, **38**, 787 – 799.

[8.] Young, R.P. Collins, D.S., Reyes-Montes, J.M., and Baker C. (2004). Quantification and interpretation of seismicity. *Int. J. Rock Mech. Min.*, **41**, 8, 1317-1327.

[9.] Chandler, N.A., Cournut, A., Dixon, D., Fairhurst, C., Hanson, F., Gray, M., Hara, K., Ishijima, Y., Kozak, E., Martino, J., Masumoto, K., McCrank, G., Sugita, Y., Thompson, P., Tillerson, J., and Vignal, B., (2002). *The Five Year Report on the Tunnel Sealing Experiment: An International Project of AECL, JNC, ANDRA and WIPP*. Atomic Energy of Canada Limited Report, AECL-12127.

[10.] AECL. (1994). *Environmental Impact Statement on the concept for disposal of Canada's nuclear fuel waste*. Atomic Energy of Canada Limited Report, AECL-10711,COG-93-1.

[11.] ASC. (2010). *InSite Seismic Processor – User Operations Manual Version 2.14d*, Applied Seismology Consultants Ltd. Shrewsbury, UK.

[12.] Urbancic, T.I., Trifu, C.-I., Mercer, R.A., Feustel, A.J., and Alexander, J.A.G. (1996). Automatic time-domain calculation of source parameters for the analysis of induced seismicity. *Bull. Seis. Soc Am*., **86**, 5.

[13.] Collins, D.S., and Young, R.P. (1997). *The Acoustic Emission and Microseismic Systems For the Tunnel Sealing Experiment: Description, Calibration, and Preliminary Analysis*, Report #RP038AECL to Atomic Energy of Canada Ltd.

[14.] Maxwell, S.C., Young R.P., Baker C., Collins, D.S., and Martin C.D. (1996). Mapping the Excavation Disturbed Zone around the Mine-by Tunnel using Induced Seismicity and Velocity Imaging. *International Conference on Deep Geological Disposal of Radioactive Waste*, Martino and Martin (eds), Canadian Nuclear Society, 67-76.

[15.] Young, R.P., Collins, D.S., Hazzard J., Pettitt, W.S. and Baker, C. (2001). *Use of acoustic emission and velocity methods for validation of micromechanical models at the URL.* Ontario Power Generation, Nuclear Waste Management Division Report, 06819-REP-01200-10060-R00.

[16.] Read, R.S. and Chandler, N.A. (2002). *An Approach To Excavation Design For A Nuclear Fuel Waste Repository – The Thermal-Mechanical Stability Study Final Report*. Ontario Power Generation, Nuclear Waste Management Division Report, 06819-REP-01200-10086-R00.

[17.] Reyes-Montes, J.M., Rietbrock, A., Collins, D.S. and Young, R.P. (2005). Relative location of excavation induced microseismicity at the Underground Research Laboratory (AECL, Canada) using surveyed reference events. *Geophys. Res. Lett*., **32**, L05308.

[18.] Reyes-Montes, J.M. and Young, R.P. (2006). Interpretation of fracture geometry from excavation induced microseismic events. In Van Cotthem, A. Charlier, R. Thimus, J.F. Tshibangu, J.P. (eds) *Multiphysics coupling and long term behaviour in rock mechanics*. Proc. intern. symp Int.Soc.Rock Mechanics., Liege, Belgium 9-12 May 2006. Rotterdam: Balkema.

[19.] Reyes-Montes, J.M. (2004). *Enhanced Spatial Resolution of MicroSeismicity in the Investigation of In-Situ Crack Interaction and Coalescence.* PhD Thesis, University of Liverpool.

[20.] Fehler, M. House, L. and Kaieda, H. (1987). Determining planes along which earthquakes occur – Method and application to earthquakes accompanying hydraulic fracturing. *J. Geophys. Res. – Solid Earth and Planets*, **92** (B9): 9407-9414.